



## Short communication

## Heat treatment effect of the Ni foam current collector in lithium ion batteries

Tae Kwon Kim, Wei Chen, Chunlei Wang\*

Department of Mechanical and Materials Engineering, Florida International University, Miami, FL 33174, USA

## ARTICLE INFO

## Article history:

Received 18 April 2011

Received in revised form 3 June 2011

Accepted 6 June 2011

Available online 12 June 2011

## Keywords:

Current collector

Anode

Heat treatment

Energy capacity

Lithium ion batteries

## ABSTRACT

Current collectors are typically electrochemically inactive in lithium ion batteries. However, they might affect the whole cell performance once they are thermally treated during battery assembly procedure. The goal of this study is to investigate the heat treatment effect of Ni foam current collectors on the electrochemical performance in lithium ion batteries. Ni foams were thermally treated at different temperatures in air, and they were characterized in terms of morphology, structure and electrochemical performance in a half cell. SEM images showed that Ni foam surface became coarse with an increase of the heating temperature. Thermally treated Ni foams below 200 °C had negligible capacity of about 0.025 mAh, but above 300 °C showed certain capacity up to 3.13 mAh at 30th cycles due to the oxide layer formed by the thermal oxidation of the Ni foam. The results demonstrate that the thermal treatment of Ni foam current collector promotes the gradual oxidation on the Ni foam surface with nonnegligible capacity contribution.

© 2011 Elsevier B.V. All rights reserved.

## 1. Introduction

During the past decades, vigorous efforts in developing more advanced lithium ion batteries have been made toward improving electrode materials which are significantly important to determine the energy capacity, power density and electrochemical potential of batteries [1]. Particularly, nanostructured electrode materials, such as nanotubes/wires, nanoparticles, nanocomposites, have demonstrated considerable improvement in the electrochemical performance due to the high electrode/electrolyte contact area, fast charge–discharge kinetics and enhanced structural stability from volume change. Typically lithium ion batteries are composed of two electrodes (i.e. anode and cathode), electrolyte, separator and current collectors. The current collectors give the electronic conduction through the active electrode materials to the external circuit without any electrochemical reactions within the operational voltage window in lithium ion batteries. Various metals such as Cu, Ni, stainless steel, are used as the current collectors in the form of thin foil, mesh or foam to improve the electrical conductivity and adhesion to active electrode materials. Among them, nickel foam has attracted great interest as current collector in fuel cells [2–4] and lithium ion batteries [5–24] due to its 3-dimensional structure, providing a larger surface area and better contact of active materials to the electrolyte.

Many different active materials are deposited on Ni foam current collectors by using different methods typically accompanying

various thermal treatments. The thermal treatments are usually conducted at temperatures ranging from room temperature to several hundred degrees Celsius under different atmosphere in order to evaporate solvents or improve crystallinity of the active materials. For example, Gille et al. casted nickel hydroxide paste on Ni foam and dried at 60 °C under vacuum to evaporate binders [5]. Huang et al. calcined NiO film on Ni foam at 350 °C in Ar after the chemical bath deposition [11–13]. Yu et al. deposited CoO, CuO and SnO<sub>2</sub> on Ni foam by Electrostatic Spray Deposition at 230–250 °C in air [17–20]. Detailed thermal treatment conditions of various fabrication methods of electrode materials on Ni foam substrate in lithium ion batteries were briefly summarized in Table 1. In all these works, however, the heat treatment effect of Ni foam current collectors on the electrochemical reaction and capacity contribution has been simply ignored. Our recent study of NiO film obtained on the Ni foam by the thermal oxidation at 500 °C showed the specific capacity up to 646 mAh g<sup>-1</sup> [23], which motivates us to study the capacity contribution of the Ni foam current collector to the total cell performance at different process temperatures. Moreover, in case of nanostructured active materials with limited weight of active materials, the capacity contribution of the oxide layer on the current collector could have considerable impact on the total cell performance. Therefore, it is important to investigate details of the thermal treatment effect of current collectors on the electrochemical performance in lithium ion batteries.

In this work, we took Ni foam current collector as an example in order to understand the heat treatment effect. Experimental efforts have been devoted to heat-treated Ni foams at different temperatures in air by characterizing their morphological, structural properties and electrochemical performance with reference

\* Corresponding author. Tel.: +1 305 348 1217; fax: +1 305 348 1932.  
E-mail address: [wangc@fiu.edu](mailto:wangc@fiu.edu) (C. Wang).

**Table 1**  
Thermal treatment conditions in different processes with Ni foam substrate.

Process method	Active material	Temperature (°C)	Heating time (h)	Atmosphere
Casting with binder	NiOOH [5]	60	1	Vacuum
	NiSb [6]	110	12	
	C-V <sub>2</sub> CVS [7]	80	24	
	Cu-Sn [8]	500	8	
	Si-Ni [9]	100	10	
	Cu <sub>2</sub> O/CuO [10]	80	–	
Electrochemical deposition	NiO [11–13]	350	2	Ar
	NiO [14]	300	0.5	
	NiO [15]	500	0.5	
	Ni <sub>2</sub> P [16]	500	1	
Electrostatic spray deposition	Cu <sub>2</sub> O/Li <sub>2</sub> O [17–18], SnO <sub>2</sub> [19]	250	3	Air
	CoO/Li <sub>2</sub> O [20]	235	2	
	Sn/CNTs [21]	200–300	1	
Vapor-phase transport	NiP <sub>2</sub> [22]	350	12	Vacuum
Thermal oxidation	NiO [23]	500	–	Air
	NiO [24]	500–700	–	

to Li metal. Our results indicate that the discharge capacities of heat-treated Ni foam were significantly affected by the heating temperatures. Their electrochemical performance showed the Ni/NiO configuration due to the thin NiO layer, either nature oxide layer or formed by the thermal oxidation during the heat treatment process, which could deliver a noticeable capacity above 300 °C. We believe the interfacial oxide layer on Ni foam can be further utilized to help us on designing new battery electrode configuration with enhanced energy density.

## 2. Experimental

Porous Ni foam (Hunan Corun New Energy) disks (16 mm in diameter) were thermally treated at different temperatures. Prior to the heat treatment, Ni foams were sonicated in the ethyl alcohol for 20 min to clean the surface of Ni foams. Then pretreated Ni foams were heated on the hot plate at temperature 100, 200, 300, 400 and 500 °C in air for 2 h, respectively (heat-treated samples are denoted as T100, T200, T300, T400, and T500). Six samples at each temperature have been prepared, and the weight difference of pretreated Ni foams before and after heating was measured. The

weight of NiO was estimated by using the method elucidated in Ref. [23].

Structural and morphological properties of heat-treated Ni foams were analyzed by X-ray diffraction (XRD) (D-5000 diffractometer; Cu K $\alpha$  radiation,  $\lambda = 0.154056$  nm) and field-emission scanning electron microscope (FESEM) (JELO, JSM 6330), respectively. Thermally treated Ni foams as a working electrode and lithium metal as counter and reference electrode were assembled in CR2032 coin cells under an argon filled glove box. The electrolyte is 1.1 M FC-130 dissolved in ethylene carbonate, dimethyl carbonate and diethyl carbonate (EC:DMC:DEC, 1:1:1 volume ratio). Cyclic voltammetric (CV) measurements were performed on a Versatile Multichannel Potentiostat (VMP3, Bio-Logic) at 0.2 mV s<sup>-1</sup> scan rate between 0.02 and 3 V (vs. Li<sup>+</sup>/Li). The galvanostatic discharge-charge cycling of cells were carried out at room temperature by using an NEWARE BTS-610 battery tester.

## 3. Results and discussion

XRD patterns of thermally treated Ni foam at different treatment temperatures are given in Fig. 1(a). Other than Ni diffraction peaks

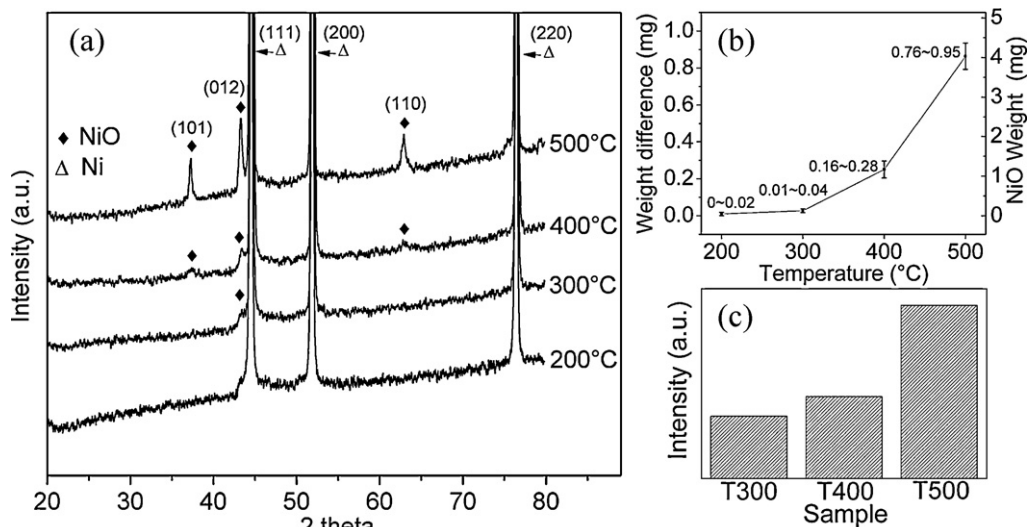


**Fig. 1.** (a) XRD patterns, (b) statistical data of Ni foam weight difference before and after heat treatment and (c) relationship of XRD peak intensity of NiO (012) plane with heating temperatures.

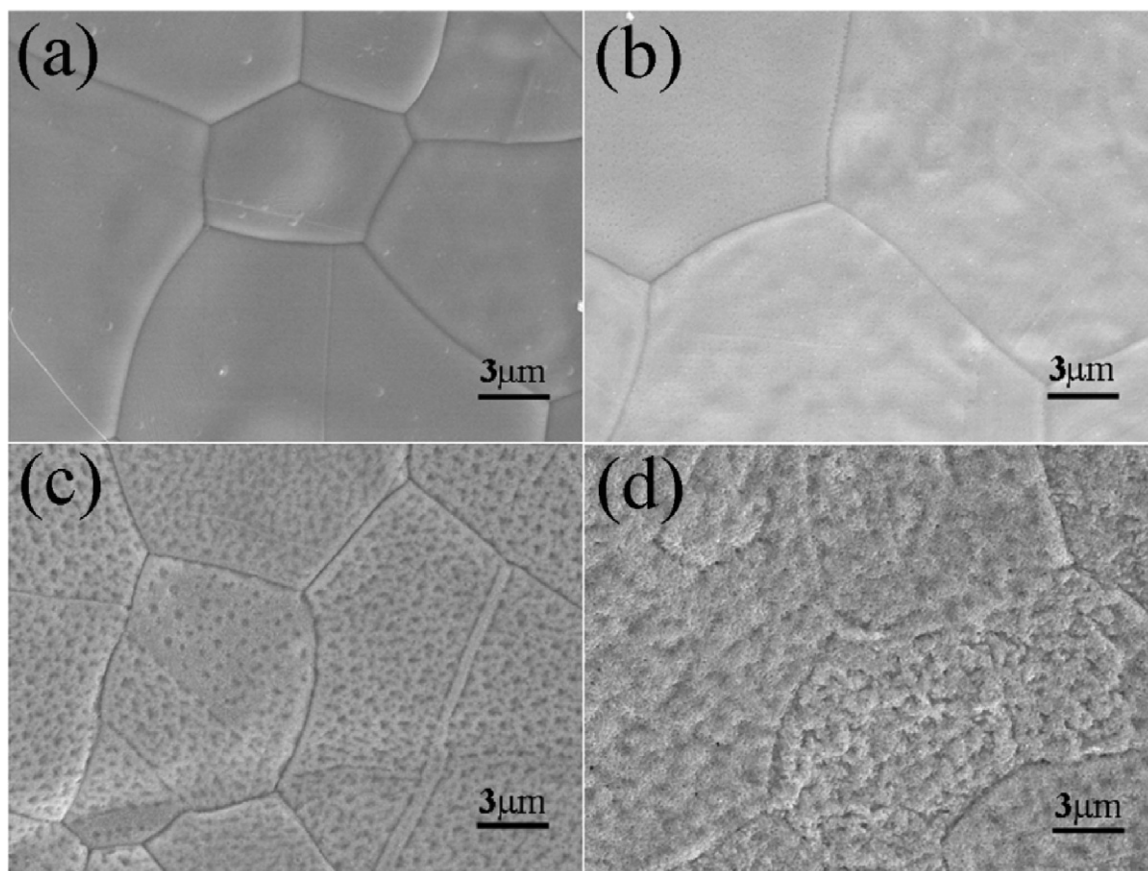


Fig. 2. SEM images of heat-treated Ni foam at (a) 200 °C, (b) 300 °C, (c) 400 °C and (d) 500 °C, respectively.

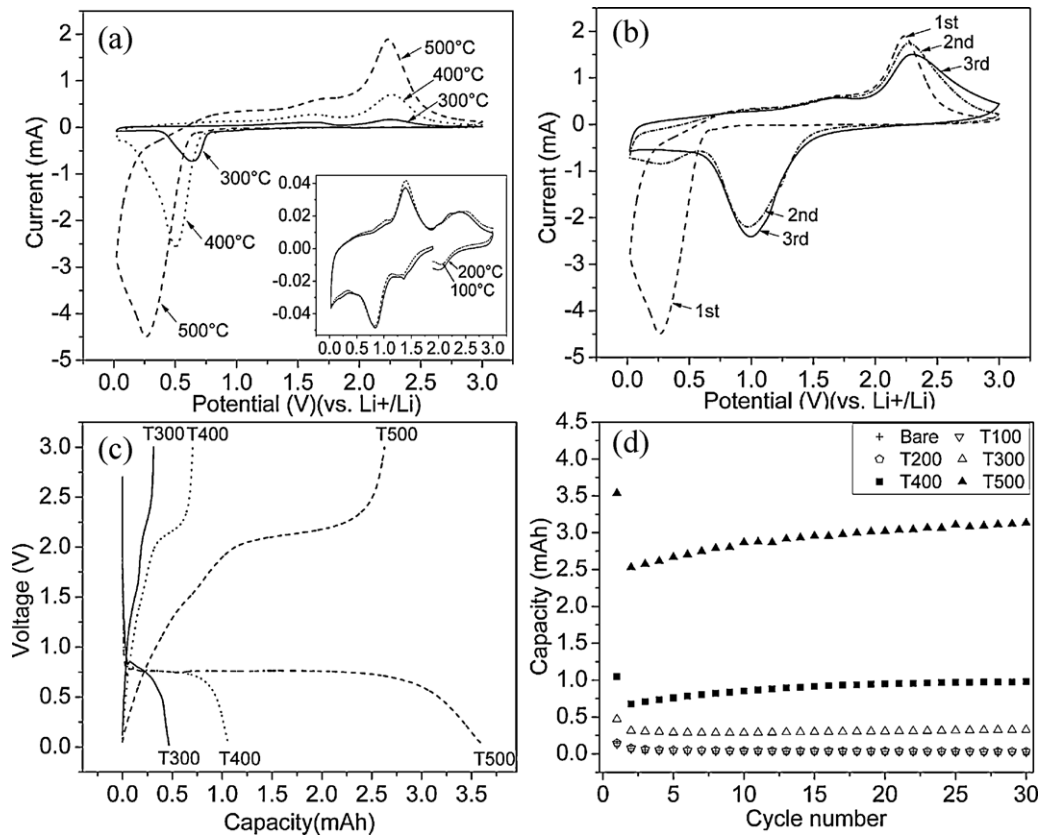
at 44.5°, 51.8° and 76.3° observed in all heat-treated Ni foams, the diffraction peaks of NiO could be mainly distinguished for samples thermally treated at above 300 °C. The three major peaks related to NiO are at  $2\theta$  of 37.2°, 43.3° and 62.9°, which are indexed to (1 0 1), (0 1 2) and (1 1 0) planes of the cubic structure NiO, respectively. Fig. 1(b) presents average weight difference before and after heat-treatment of samples from 100 to 500 °C. It can be found that the weight difference is negligible below 300 °C, and it is increasing with the increase of temperature at 300–500 °C. The average weight difference at 500 °C reached 0.86 mg corresponding to NiO weight of 4.01 mg if we simply assume the oxide layer is uniform in depth. Fig. 1(c) shows the NiO (0 1 2) plane peak intensity for samples thermally treated above 300 °C. The intensity of NiO diffraction peak becomes stronger with increase of the heat treatment temperature, corresponding to the weight difference of Ni foam before and after heat treatment in Fig. 1(b). The increase of both XRD peak intensity and weight difference indicates the gradual NiO film growth from the thermal oxidation of the Ni foam surface.

Fig. 2 shows SEM pictures of heat-treated Ni foam surfaces at 200, 300, 400 and 500 °C, respectively. Different surface morphologies of heat-treated Ni foam were formed at different heat treatment temperatures. Sample T200 (Fig. 2(a)) shows the relatively smooth surface with legible grain boundaries. The smooth surface of each grain became rough with the increase of the heating temperature due to the oxidation of Ni into NiO (Fig. 2(b)). Moreover, uniformly distributed fine irregular-shaped features around 200 nm in diameter gradually appeared at 400 °C (Fig. 2(c)), and they further grew on the surface until the grain boundaries became unclear at 500 °C (Fig. 2(d)). The morphology change of Ni foam surface was strongly influenced by the heat treatment temperature. The surface of Ni foam was oxidized via a gas–solid thermal

reaction forming gradually an integrated Ni/NiO structure. The thickness and density of the oxide layer depends mainly on two heat treatment parameters, i.e., oxidation time and temperature. In this study, all the samples were heat-treated for 2 h, so the higher the temperature the thicker and denser the NiO layer has been formed.

In Fig. 3(a), the 1st cycle CV profiles of heat-treated Ni foams at different temperatures show that as heat treatment temperature increases, the cathodic peak of the 1st cycle shifts to lower voltage from 0.8 V for T300, to 0.5 V for T400, and 0.25 V for T500 gradually, corresponding to the initial reduction reaction of NiO to Ni layer and the formation of a solid electrolyte interface (SEI). For T100 and T200, the peak currents are considerably low compared to T300, T400 and T500, which indicates the negligible capacity contribution due to the thin or partially oxidized NiO layer on Ni foam at low temperature treatment, but the zoom in result shows similar Ni/NiO electrochemical configuration in the insert of Fig. 3(a). For T500, the cathodic peak becomes broad and weak after 1st cycle and shifts to around 1 V in the subsequent cycles as presented in Fig. 3(b) due to the SEI formation, mainly occurred at 1st cycle. In the anodic scan, two broad peaks at around 1.6 V and 2.2 V were resolved, attributed to the decomposition of the partially reversible polymeric coating on the NiO surface and  $\text{Li}_2\text{O}$ , respectively [25–28].

The 1st cycle voltage vs. capacity profiles (i.e., charge–discharge curves) of heat-treated Ni foams in the voltage range of 0.02–3.0 V at a constant current of 0.05 mA were plotted in Fig. 3(c). Ni foam T100 and T200 electrodes (not shown here) only deliver capacity of 0.13 and 0.14 mAh in 1st cycle. Heat-treated Ni foams at over 300 °C, T300, T400 and T500, have the typical discharge characteristics of NiO with a long voltage plateau at about 0.7 V by a sloping discharge curve down to the cut-off voltage of 0.02 V during 1st



**Fig. 3.** (a) Cyclic voltammetry curves of heat-treated Ni foams at the 1st cycle at different heating temperatures, (b) cyclic voltammetry curves of T500 sample from the 1st to 3rd cycles, the CV curves of each heat-treated Ni foam were recorded in potential window of 0.02 to 3 V (vs. Li) at  $0.2 \text{ mV s}^{-1}$  scan rate. (c) 1st cycle charge–discharge profile, and (d) cyclability of samples treated at different temperatures, recorded at constant current of 0.05 mA.

cycle delivering capacity of 0.46, 1.06 and 3.61 mAh, respectively. Moreover, the corresponding specific capacities of T400 and T500 are  $1088$  and  $1021 \text{ mAh g}^{-1}$ , respectively, which were calculated based on the weight differences of Ni foams before and after the heat treatment for T400 and T500. The discharge plateaus are well corresponding to the respective cathodic peak observed in the CV curves, shown in Fig. 3(a). The irreversible capacity loss during 1st cycle of the heat-treated Ni foam is gradually decreased from 47% at  $100^\circ\text{C}$  to 27% at  $500^\circ\text{C}$ , indicating better reversibility at higher temperatures. We believe that the high irreversible capacities of low temperature heat-treated samples, T100 and T200, in 1st cycle might be attributed to the negligible conversion reaction of NiO to Ni, and most of capacities might come from the formation of the solid electrolyte and decomposition of the incomplete  $\text{Li}_2\text{O}$ .

The cycling performance of heat-treated Ni foams was examined, as displayed in Fig. 3(d). The results revealed that the capacities of bare Ni foam, T100 and T200 are very limited (around 0.025 mAh) and exhibit similar retention within 30 cycles. While the capacities at 30th cycle of T300, T400 and T500 show 0.32, 0.97 and 3.13 mAh, respectively, indicating the capacity increases with the increase of heat treatment temperatures. The specific capacities of T400 and T500 were estimated based on the calculated NiO weight as  $998$  and  $885 \text{ mAh g}^{-1}$ , respectively, showing the capacities are higher than the theoretical one of NiO ( $718 \text{ mAh g}^{-1}$ ). This may be attributed to the partially reversible polymer-like SEI coating, formed by the electrolyte decomposition [26,29,30]. Especially, the high specific capacity of T400 might come from the high surface area of the porous morphology interfacial layer which benefits the interaction reaction of active materials with electrolyte and reduce  $\text{Li}^+$  diffusion path [20,31]. From the results of Ni foam heat treatment effect on the electrochemical performance, we can conclude

that (1) the electrochemical performance of the heat-treated Ni foam was strongly influenced by the heat treatment temperatures; (2) the interfacial oxide layer contributes nonnegligible capacity to the whole cell performance above  $300^\circ\text{C}$ . The capacity contribution of the Ni/NiO configuration is directly related to the morphology change and the amount of the oxide layer formed on the Ni surface. The improved energy capacity and good cyclability for samples treated above  $300^\circ\text{C}$  are due to the unique Ni/NiO structure which offers good adhesion, better kinetics, and negligible contact resistance between active NiO anodes and the underlying inactive Ni current collector. Moreover, the porous nature of the Ni/NiO configuration could buffer volume expansion/constriction which usually leads to the pulverization and degradation of the transition metal oxide electrodes during the conversion reactions. Further research needs to be done to assemble the anode electrodes with typical cathodes to build full cells and examine the level of contribution of various types of current collectors to the battery performance. It should be noted that the oxide interfacial layers could be used to design better battery electrode configurations with enhanced energy capacities.

#### 4. Conclusions

The thermal treatment effect of Ni foam current collector on the electrochemical performance was investigated. NiO layer was gradually grown on the Ni foam surface with the increase of the heating temperature. The capacity contributions were confirmed nonnegligible at heat treatment temperatures above  $300^\circ\text{C}$ . Therefore, it demonstrates that the thermal treatment promotes gradual oxidation of the Ni foam surface with increased temperatures, which

could be applied to more advanced battery electrode design with improved energy capacities.

### Acknowledgements

The authors would like to acknowledge American Chemical Society (Petroleum Research Fund, 49301-0N110), and the Advanced Materials Engineering Research Institute (AMERI) facility and Florida International University.

### References

- [1] J.M. Tarascon, N. Reham, M. Armand, *Chem. Mater.* 22 (2010) 724–739.
- [2] D. Cao, Y. Gao, G. Wang, R. Miao, Y. Liu, *Int. J. Hydrogen Energy* 35 (2010) 807–813.
- [3] X.Z. Fu, J. Melnik, Q.X. Low, J.L. Luo, K.T. Chuang, A.R. Sanger, Q.M. Yang, *Int. J. Hydrogen Energy* 35 (2010) 11180–11187.
- [4] W. Yang, S. Yang, W. Sun, G. Sun, Q. Xin, *Electrochim. Acta* 52 (2006) 9–14.
- [5] G. Gille, S. Albrecht, J.M. Markscheffel, A. Olbrich, F. Schruppf, *Solid State Ionics* 148 (2002) 269–282.
- [6] J. Xie, X.B. Zhao, H.M. Yu, H. Qi, G.S. Cao, J.P. Tu, *J. Alloys Compd.* 441 (2007) 231–235.
- [7] Y. Zhang, X. Wu, H. Feng, L. Wang, A. Zhang, T. Xia, H. Dong, *Int. J. Hydrogen Energy* 34 (2009) 1556–1559.
- [8] M. Yao, K. Okuno, T. Iwaki, T. Awazu, T. Skai, *J. Power Sources* 195 (2010) 2077–2081.
- [9] X. Wang, Z. Wen, Y. Liu, *Electrochim. Acta* 56 (2011) 1512–1517.
- [10] Q. Pan, M. Wang, Z. Wang, *Electrochem. Solid-State Lett.* 12 (3) (2009) A50–A53.
- [11] X.H. Huang, J.P. Tu, X.H. Xia, X.L. Wang, J.Y. Xiang, *Electrochem. Commun.* 10 (2008) 1288–1290.
- [12] X.H. Huang, J.P. Tu, X.H. Xia, X.L. Wang, J.Y. Xiang, L. Zhang, Y. Zhou, *J. Power Sources* 188 (2009) 558–591.
- [13] X.H. Huang, J.P. Tu, X.H. Xia, X.L. Wang, J.Y. Xiang, L. Zhang, *J. Power Sources* 195 (2010) 1207–1210.
- [14] H. Wang, Q. Pan, X. Wang, G. Yin, J. Zhao, *J. Appl. Electrochem.* 39 (2009) 1597–1602.
- [15] Q. Pan, J. Liu, *J. Solid State Electrochem.* 13 (2009) 1591–1597.
- [16] J.Y. Xiang, J.P. Tu, X.L. Wang, X.H. Huang, Y.F. Yuan, X.H. Xia, Z.Y. Zeng, *J. Power Sources* 185 (2008) 519–525.
- [17] Y. Yu, C.H. Chen, J.L. Shui, S. Xie, *Angew. Chem. Int. Ed.* 44 (2005) 7085.
- [18] Y. Yu, Y. Shi, C.H. Chen, C. Wang, *J. Phys. Chem.* 112 (2008) 4176–4179.
- [19] Y. Yu, L. Gu, A. Dhanabalan, C.H. Chen, C. Wang, *Electrochim. Acta* 54 (2009) 7227–7230.
- [20] Y. Yu, C.H. Chen, J.L. Shui, S. Xie, *Angew. Chem.* 117 (2005) 7247–7251.
- [21] A. Dhanabalan, Y. Yu, X. Li, K. Bechold, C. Wang, *J. Mater. Res.* 25 (2010) 1554–1560.
- [22] F. Gillot, S. Boyanov, L. Dupont, M.L. Doublet, M. Morcrette, L. Monconduit, J.M. Tarascon, *Chem. Mater.* 17 (2005) 6327–6337.
- [23] X. Li, A. Dhanabalan, K. Bechtold, C. Wang, *Electrochem. Commun.* 12 (2010) 1222–1225.
- [24] C. Wang, D. Wang, Q. Wang, H. Chen, *J. Power Sources* 195 (2010) 7432–7437.
- [25] S. Grugeon, S. Laruelle, R. Herrera-Urbina, L. Dupont, P. Poizot, J.M. Tarascon, *J. Electrochem. Soc.* 148 (2001) A285.
- [26] A. Debart, L. Dupont, P. Poizot, J.B. Leriche, J.M. Tarascon, *J. Electrochem. Soc.* 148 (2001) A1266.
- [27] S. Laruelle, S. Grugeon, P. Poizot, M. Dolle, L. Dupont, J.M. Tarascon, *J. Electrochem. Soc.* 149 (2002) A627.
- [28] M. Dolle, P. Poizot, L. Dupont, J.M. Tarascon, *Electrochem. Solid-State Lett.* 5 (2002) A18.
- [29] X.H. Huang, J.P. Tu, B. Zhang, C.Q. Zhang, Y. Li, Y.F. Yuan, H.M. Wu, *J. Power Sources* 161 (2006) 541–544.
- [30] S.A. Needham, G.X. Wang, H.K. Liu, *J. Power Sources* 159 (2006) 254–257.
- [31] M. Yao, K. Okuno, T. Iwaki, M. Kato, S. Tanase, K. Emura, T. Sakai, *J. Power Sources* 173 (2007) 545.